Pergamon

SCIENCE DIRECT®

Tetrahedron 59 (2003) 6027–6034

TETRAHEDRON

Structure and isomerization in 4,4′-biimidazoles: a comparison of crystal structures and theoretical calculations of 2,2′-dimethyl-4,4′-biimidazole and 2,2′-dimethyl-4,4′-biimidazolium bis-trifluoroactate

Weidong Zhang,[a] Christopher P. Landee,[b] Roger D. Willett[c] and Mark M. Turnbull[a,d,*]

[a]*Carlson School of Chemistry and Biochemistry, Clark University, 950 Main St., Worcester, MA 01610, USA*
[b]*Department of Physics, Clark University, 950 Main St., Worcester, MA 01610, USA*
[c]*Department of Chemistry, Washington State University, Pullman, WA, USA*
[d]*Department de Química Física, Facultat de Química, Universitat de Barcelona, Av. Diagonal 647, 08028 Barcelona, Spain*

Received 8 May 2003; revised 24 June 2003; accepted 24 June 2003

Abstract—The crystal structures of the compounds 2,2′-dimethyl-4,4′-biimidazole dihydrate (**1**) and 2,2′-dimethyl-4,4′-biimidazolium bistrifluoroacetate (**2**) have been determined. Compound **1** is linked into a three dimensional network via hydrogen bonding between the imidazole nitrogens and the water molecules, while compound **2** forms sheets through hydrogen bonding between the acetate and imidazolium ions. Theoretical calculations for **1** show that the particular prototropic tautomer observed in the crystal structure is not the lowest energy isomer. This observation is justified in terms of hydrogen bonding to the lattice water molecules.

1. Introduction

For close to two decades, the molecular magnetism community has been interested in the design and synthesis of site-ordered bimetallic coordination complexes.[1] Early work by Decurtins,[2] Kahn[3] and Okawa[4] among others demonstrated successful routes to the synthesis of one-, two- and three-dimensional coordination polymers through the use of careful ligand design. We have been interested in the development of such systems and are especially interested in the use of polyazoles to produce related bimetallic complexes.[5] The compound 4,4′-biimidazole and its derivatives can be used for the preparation of such complexes due to its three potential binding sites when in the *S-cis* conformation (see Fig. 1).

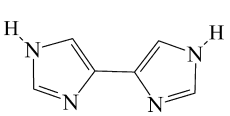

4,4'-Biimidazole

Removal of the two N–H protons generates a dianion with a chelating site to bind a metal ion, and two additional nitrogen atoms that can coordinate to additional metal ions and extend the complex into a coordination polymer. The use of bridging imidazoles to propagate magnetic exchange is particularly attractive since imidazoles, as the imidazolate ion, are known to mediate magnetic exchange as high as 200 cm^{-1}.[6] The isomer 2,2′-biimidazole is well known and the structure of the neutral base[7] and its hydrochloride salt[8]

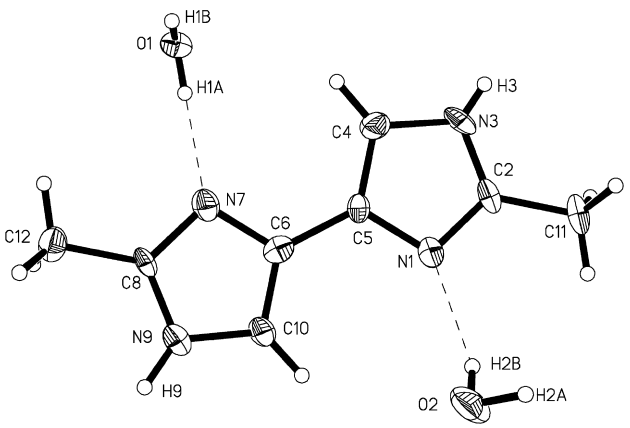

Figure 1. Thermal ellipsoid plot of the asymmetric unit of compound **1**. Hydrogen atoms are shown as spheres of arbitrary size and only those hydrogens whose positions were refined are labeled.

Keywords: 4,4′-biimidazole; crystal structures; hydrogen bonding.
* Corresponding author. Address: Carlson School of Chemistry and Biochemistry, Clark University, 950 Main St., Worcester, MA 01610, USA. Tel.: +1-508-793-7167; fax: +1-508-793-8861;
e-mail: mturnbull@clarku.edu

0040–4020/$ - see front matter © 2003 Elsevier Ltd. All rights reserved.
doi:10.1016/S0040-4020(03)00987-6

have been reported, as have first row transition metal complexes of the neutral,[9] mono-[9a,b,10] and di-deprotonated species.[10b,11]

The potential for 4,4′-biimidazole and its derivatives to serve as bridging ligands for two-dimensional transition metal complexes as described above will be highly dependant upon the structure of the molecule. Most important will be the ability to chelate a single metal ion in an *S-cis* conformation, allowing the remaining nitrogen atoms to bridge to two different metal ions (unlike 2,2′-biimidazole where two chelating sites are formed, limiting bridging structures to chains). Thus we have examined the structure of 2,2′-dimethyl-4,4′-biimidazole (as the dihydrate, **1**) and its trifluoroacetate salt (**2**) both via X-ray diffraction and computational studies.

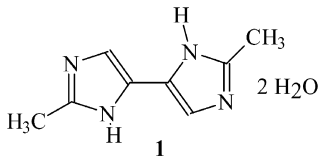

1

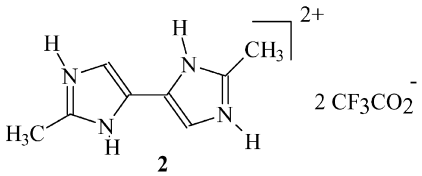

2

2. Results

Synthesis. Compound **2** was prepared according to literature procedures[12] and converted to the neutral dihydrate **1** by reaction with NaOH in aqueous solution at room temperature. Their structures were determined by single crystal X-ray crystallography (see Table 1 for data collection and refinement parameters). The asymmetric unit of **1** is shown in Figure 1. Bond lengths and angles are given in Table 2.

Compound **1** crystallizes as the dihydrate in the monoclinic space group Cc. The molecule is in the *S-trans* conformation and there is a pseudo-inversion center mid-way along the C5–C6 bond, but the symmetry is broken by the different positions and hydrogen bonding characteristics of the water molecules, as well as small changes in bond lengths and angles remote to the ring junction. Symmetry equivalent bond lengths within **1** are the same within experimental error except for the C2–N3/C8–N9 pair where the latter is significantly longer (1.316(6) and 1.339(6) Å respectively) and the N3–C4/N9–C10 bond where the latter is comparably shorter (1.391(6) and 1.368(7) Å respectively). The two imidazole rings are planar (mean deviation 0.0013 Å for the N1 ring; 0.0012 for the N7 ring) and the methyl groups lie nearly in their respective planes (0.012 for C11; −0.008 Å). The angles within the rings vary greatly. The C–N–C angles (range ~105–108°) and the intra-ring N–C–$C_{ring\ junction}$ angles (mean=105.7(6)) are the smallest while the inter-ring C–C–C angles are near 128°. The angle between the mean planes of the rings is 6.4°, as a result of both a ring twisting and a slight folding of the molecule along the C5–C6 bond as the torsion angles C4–C5–C6–N7 (4.6(7)°) and N1–C5–C6–C10 (6.1(7)°) differ slightly. The first structure reported containing the 4,4′-biimidazole moiety was the 3-(2-imidazolyl)-*N*,*N*-sulfone bridged compound.[13] The imidazole rings are nearly perpendicular in this compound (dihedral angle between rings=78.6°) precluding conjugation and the C5–C6 bond is slightly longer (~0.01 Å) compared to **1** as a result.

Hydrogen bonds link molecules of **1** related by C-centering into puckered sheets (see Fig. 2). The 4,4′-biimidazole molecules are initially linked into chains by hydrogen bonding interactions between the imidazoles and the water molecules. These chains are then linked into the sheets via H-bonds between the water molecules. The strongest of these hydrogen bonds (based upon distance and angle criteria) occur between N3–H3···O2 [$d_{N3\cdots O2}$=2.765(6); $\angle_{N3-H3\cdots O2}$=174(6)°] and O1–H1A···N7 [$d_{O1\cdots N7}$=2.747(5); $\angle_{O1-H1A\cdots N7}$=178(5)°]. The refined position of H3 results in an unusually short N–H bond [0.73(6) Å]. This may result from the very short N3···O2 separation and is not necessarily an accurate representation of the position of H3.

The sheets are then linked into a three-dimensional network by a somewhat weaker hydrogen bond between O1 and N1A (symm. transform: x+0.5, y+0.5,z). Details of the hydrogen bonds and their calculated interaction energies are given in Table 3a.

Biimidazolium salt **2** crystallized in the tetragonal space group *I*-42*d*. The asymmetric unit is shown in Figure 3. As was the case for **1**, compound **2** crystallizes in the *S-trans* conformation and contains a pseudo-inversion center mid-way along the C5–C6 bond.

The two halves of the biimidazolium ion in **2** are more nearly identical than was the case for **1**. Symmetry equivalent bond lengths within **2** are the same within experimental error except for the C2–C11/C8–C12 pair (1.480(4) and 1.497(4) Å respectively). The same is true for bond angles with only four pairs of angles differing by more than experimental error. The individual imidazole rings are less planar than in **1** (mean deviation 0.0069 Å for the N1 ring; 0.0082 for the N7 ring) and the methyl groups lie further out of their respective planes (0.032 for C11; −0.017 Å for C12). The ion as a whole, however, is more planar; the angle between the mean planes of the rings is 0.9°.

The trifluoroacetate ions exhibit three-site disorder for the CF_3 groups via rotation about the C21–C22 and C31–C32 bonds. The trifluoromethyl groups were refined with restraints for the C–F bondlengths and the F···F interatomic distances to maintain nearly tetrahedral geometry. In both trifluoroacetate ions, the final refinement showed approximately 50% occupancy for one CF_3 rotomer, with the remaining occupancy divided~2.5:1 between the remaining sites.

Table 1. Crystal data and structure refinement for 2,2′-dimethyl-4,4′-biimidazole (**1**) and 2,2′-dimethyl-4,4′-biimidazolium bistrifluoroacetate (**2**)

	1	**2**
Empirical formula	$C_8H_{14}N_4O_2$	$C_{12}H_{12}F_6N_4O_4$
Formula weight	198.23	390.26
Temperature	168(2) K	173(2) K
Crystal system	Monoclinic	Tetragonal
Space group	Cc	*I*-42*d*
Unit cell dimensions	a=7.291(3) Å	a=21.824(4) Å
	b=12.269(7) Å	b=21.824(4) Å
	c=11.525(6) Å	c=13.676(3) Å
	α=90°	α=90°
	β=95.336(14)°	β=90°
	γ=90°	γ=90°
Volume	1026.5(9) Å^3	6514(2) Å^3
Z	4	16
Density (calculated)	1.283 Mg/m^3	1.592 Mg/m^3
Absorption coefficient	0.095 mm^{-1}	0.163 mm^{-1}
F(000)	424	3168
Crystal size	0.44×0.39×0.36 mm^3	0.56×0.34×0.21 mm^3
Theta range for data collection	3.26–26.36°	2.56–24.71°
Index ranges	$-7\leq h\leq 3$	$-25\leq h\leq 25$
	$-15\leq k\leq 15$	$-25\leq k\leq 25$
	$-13\leq l\leq 14$	$-16\leq l\leq 8$
Reflections collected	2227	36708
Independent reflections	1165 [R(int)=0.0318]	2778 [R(int)=0.0647]
Completeness to theta	26.36° (90.3%)	24.71° (99.9%)
Absorption correction	Empirical from equivalents	
Max. and min. transmission	1.0000 and 0.5593	1.0000 and 0.6346
Refinement method	Full-matrix least-squares on F^2	
Data/restraints/parameters	1165/2/146	2778/146/363
Goodness-of-fit on F^2	1.119	1.027
Final R indices [$I>2\sigma(I)$]	R1=0.0588, wR2=0.1336	R1=0.0360, wR2=0.0916
R indices (all data)	R1=0.0640, wR2=0.1363	R1=0.0657, wR2=0.1087
Extinction coefficient	0.015(3)	0.00021(6)
Largest diff. peak and hole	0.303 and −0.297 eÅ^{-3}	0.235 and −0.178 eÅ^{-3}

Compound **2** is linked into layers parallel to the C-face, stabilized by hydrogen bonding (see Fig. 4). Each trifluoroacetate bridges two 4,4′-biimH_2 ions via one endo N–H and one exo N–H ($d_{N\cdots O}$~2.7 Å; see Table 3b).

This results in the formation of two types of cavities in the layer, one cavity surrounded by methyl groups from the biimidazole (~4.5 Å in diameter) and a small second cavity surrounded by the CF_3 groups (~1.5 Å in diameter). The van der Waals radii of the neighboring atoms (H or F) were subtracted from the interatomic distances in both cases. Successive layers are related by alternating two-fold rotation axes parallel to the *ab*-plane so that the two types of cavities alternate parallel to the *c*-axis; uniform channels

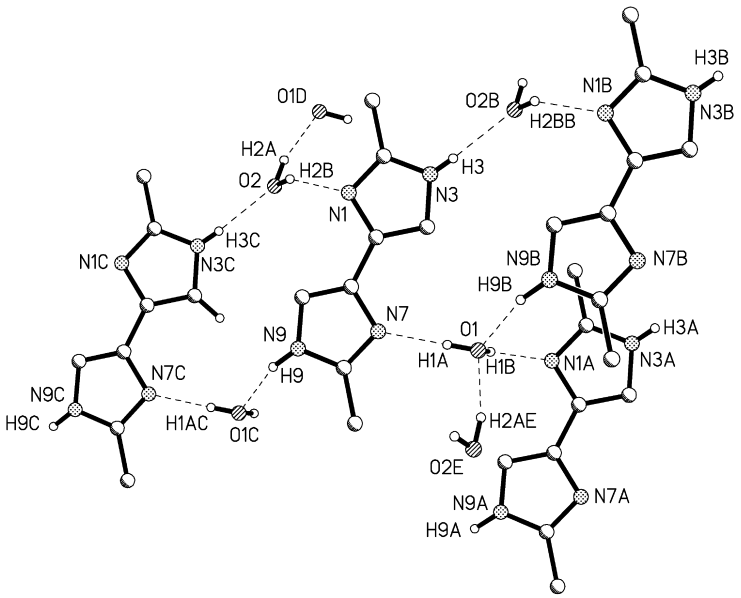

Figure 2. Partial packing diagram of **1**. Dotted lines represent hydrogen bonds. Hydrogen atoms not involved in hydrogen bonding have been excluded for clarity.

Table 2. Bond lengths [Å] and angles [°] for **1** and **2**

Bond	1	2	Angle	1	2
N1–C2	1.329(6)	1.336(3)	C2–N1–C5	104.8(4)	109.3(2)
N1–C5	1.386(6)	1.387(3)	N3–C2–N1	112.2(5)	107.6(2)
C2–N3	1.316(6)	1.343(3)	N3–C2–C11	123.3(5)	126.7(2)
C2–C11	1.501(7)	1.480(4)	N1–C2–C11	124.5(5)	125.7(2)
N3–C4	1.391(7)	1.381(3)	N1–C5–C6	121.6(4)	122.30(18)
C4–C5	1.365(7)	1.359(3)	C2–N3–C4	108.2(4)	109.30(19)
C5–C6	1.464(6)	1.453(3)	C5–C4–N3	104.7(4)	106.9(2)
C6–C10	1.348(7)	1.366(3)	C4–C5–N1	110.1(4)	106.8(2)
C6–N7	1.378(6)	1.388(3)	C4–C5–C6	128.3(4)	130.9(2)
N7–C8	1.336(6)	1.328(3)	C6–C10–N9	106.7(4)	107.0(2)
C8–N9	1.339(6)	1.340(3)	C10–C6–N7	109.9(5)	106.2(2)
C8–C12	1.500(7)	1.497(4)	C10–C6–C5	128.6(4)	131.10(19)
N9–C10	1.368(7)	1.387(3)	N7–C6–C5	121.4(4)	122.72(17)
			C8–N7–C6	104.8(4)	109.8(2)
			N7–C8–N9	111.5(5)	108.0(2)
			N7–C8–C12	125.1(4)	125.9(2)
			N9–C8–C12	123.5(5)	126.1(2)
			C8–N9–C10	107.2(4)	109.0(2)
O21–C21		1.249(3)	O22–C21–O21		129.7(2)
O22–C21		1.229(3)	O22–C21–C22		117.5(2)
C21–C22		1.547(4)	O21–C21–C22		112.8(2)
C22–F23		1.322(10)	F23–C22–F21		108.7(8)
C22–F21		1.325(8)	F23–C22–F22		105.1(6)
C22–F22		1.385(9)	F21–C22–F22		104.3(6)
			F23–C22–C21		111.8(8)
			F21–C22–C21		115.8(4)
			F22–C22–C21		110.4(6)
O31–C31		1.256(3)	O32–C31–O31		129.3(2)
O32–C31		1.244(3)	O32–C31–C32		115.3(2)
C31–C32		1.543(3)	O31–C31–C32		115.3(2)
C32–F31		1.376(7)	F33–C32–F32		108.3(7)
C32–F32		1.333(8)	F33–C32–F31		106.3(5)
C32–F33		1.313(8)	F32–C32–F31		106.5(6)
			F33–C32–C31		110.0(6)
			F32–C32–C31		115.3(5)
			F31–C32–C31		110.0(5)

Only one representative set of data is included for each disordered trifluoromethyl group.

are not formed. This packing motif is most likely adopted to minimize the ionic repulsion that would occur if the trifluoroacetate anions were aligned one atop the next.

Successive layers parallel to the *c*-axis show alternating close contacts between the 4,4′-biimH_2 ions (see Fig. 5). 4,4′-BiimH_2 ions related by the two-fold axis parallel to *a* have their closest contacts between symmetry related atoms (C5–C5B, C10–C10B) while 4,4′-biimH_2 ions related by the two-fold axis parallel to *b* show a pair of identical contact distances between the bridging carbons (C5–C6A, C6–C5A). Mean planes of adjacent rings are nearly parallel with dihedral angles between them ranging from ~1–7°.[14]

Modeling studies and calculations. 2,2′-Dimethyl-4,4′-biimidazole can exist as three different tautomers each having two planar conformations (Fig. 6). The conformations are distinguished by the relative positions of the nitrogen atoms adjacent to the ring junction (*S-cis* or *S-trans*) and the tautomers are distinguished by the positions of the hydrogen atoms bonded to nitrogen using the same numbering scheme as was used in the crystal structure. This gives six different structures, three *S-trans* forms **1a**–**1c** (1,7-*S-trans*, 1,9-*S-trans* and 3,9-*S-trans* respectively) and three conformationally related *S-cis* forms **1d**–**1f** (1,7-*S-cis*, 1,9-*S-cis* and 3,9-*S-cis* respectively) (note that two possible isomers are equivalent to two others by symmetry reducing the eight possible isomers to six). Geometry optimizations were carried out on **1a**–**f** at the RHF level using the 3-21G basis set. Then RB3LYP/3-21G* single point energy calculations were carried out on the optimized structures and on data obtained directly from the crystal structure of **2** (unoptimized). The results from the calculations on **1a**–**f** are given in Table 4 with the energies normalized to the optimized structure energy for **1c**, the isomer that is observed in the crystal structure of **1**. Hydrogen bonding energies (Table 3a) were determined as the energy difference between individual 4,4′-biim/water or water/water pairs using the crystallographic coordinates (unoptimized structures) and the energy for the same pairs separated by an additional 100 Å. The calculated values for the hydrogen bonds are within the expected ranges and representative of the individual molecular pairs only (cooperativity effects within larger aggregates will play significant roles in the energy of the lattice as a whole).

To determine interaction energies for compound **2**, a single point energy calculation was performed on the asymmetric unit using the crystal data. Then the interaction energies within the layer were investigated by adding successive asymmetric units, in their crystallographic positions, until the cavities were generated, once for the CH_3-lined cavity and once for the CF_3-lined cavity. These energies were then compared to the energy for the same number of independent asymmetric units to determine the stabilization energy for the interaction between units within the plane. The results are presented in Table 5.

Table 3b. Hydrogen bonds for **2** [Å and °]

D–H···A	*d*(D–H)	*d*(H···A)	*d*(D···A)	<(DHA)
N(1)–H(1)···O(21)	0.97(3)	1.68(3)	2.636(3)	167(2)
N(7)–H(7)···O(31)	0.94(3)	1.75(3)	2.671(3)	169(3)
N(3)–H(3)···O(22)#1	0.81(2)	1.95(2)	2.765(2)	179(6)
N(9)–H(9)···O(32)#2	0.83(2)	1.92(2)	2.750(3)	175(6)

Symmetry transformations used to generate equivalent atoms :#(1) *y*—1,−*x*+1,−*z*+2 #(2) *y*,−*x*+1,−*z*+2.

Table 3a. Hydrogen bonds for **1** [Å and °]

D–H···A	*d*(D–H)	*d*(H···A)	*d*(D···A)	<(DHA)	E_{calc} (kcal/mol)
N(3)–H(3)···O(2)#1	0.73(6)	2.03(6)	2.765(6)	174(6)	−6.66
N(9)–H(9)···O(1)#2	0.93(6)	1.95(6)	2.855(6)	163(5)	−7.36
O(1)–H(1A)···N(7)	0.83(6)	1.92(6)	2.747(5)	178(5)	−10.28
O(1)–H(1B)···N(1)#3	0.80(6)	2.15(6)	2.876(5)	152(5)	−5.92
O(2)–H(2A)···O(1)#4	0.89(7)	1.94(7)	2.812(5)	166(6)	−7.59
O(2)–H(2B)···N(1)	0.81(8)	2.16(8)	2.898(6)	153(8)	−6.77

Symmetry transformations used to generate equivalent atoms :#(1) *x*—1/2,*y*+1/2,*z* #(2) *x*+1/2,*y*—1/2,*z* #(3) *x*+1/2,*y*+1/2,*z* #(4) *x*—1/2,−*y*+3/2,*z*—1/2.

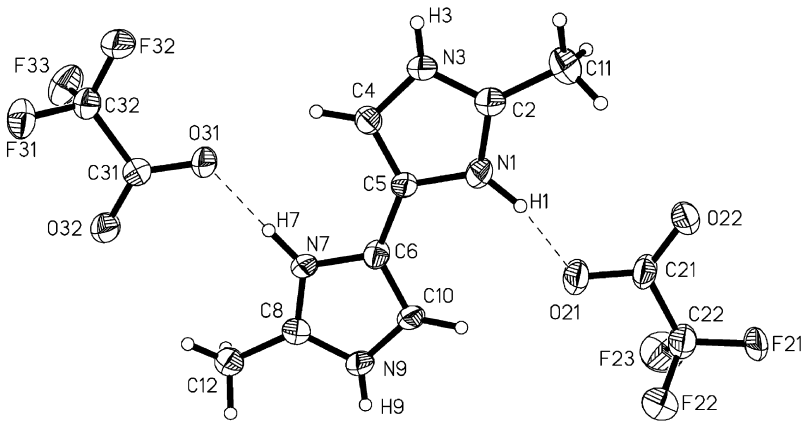

Figure 3. Thermal ellipsoid plot of **2**. Hydrogen atoms are shown as spheres of arbitrary size and only those hydrogens whose positions were refined are labeled. Only one relative position for each disordered CF_3 group is shown.

3. Discussion

Little has been reported about the synthesis and properties of 4,4′-biimidazoles[15] and the parent compound was unknown until Pyne's report in 1994.[12] Recently, Morita et al. reported an alternative synthesis for the parent and some related oligomers, including the structure of a hydrated cocrystal of 4,4′-biimidazole with its monohydrochloride salt.[16] The structures of **1** and **2** both show fundamentally planar biimidazole systems linked into two-dimensional extended sheets via hydrogen bonding. The deviations from co-planarity for the two compounds are both small, but significantly smaller in the biimidazolium dication of **2** (6.4 and 0.9° respectively). This can be compared with Morita's structure where the monoprotonated 4,4′-biimidazolium ions are also nearly planar (~5.0°), but where the neutral molecules show torsion angles of ~20.3°.[16] The twist about the central C–C bond in 4,4′-biimidazole is surprising since the molecule adopts the conformation shown in **1c**, the same as compound **1**, which is calculated to have a planar structure Diprotonation of the 4,4′-biimidazole induces lengthening of the C2–N3, C6–C10 and N9–C10 bonds by ~0.02 Å and shortens the C2–C11 bond in **2** relative to **1**. More significant changes are observed in the bond angles. The angles at the protonated nitrogens have increase by ~5° while the N–C–N bond angles have decreased by ~4°. The endocyclic C–C–N angles at the ring junctions have decreased by ~3°. Other changes in bond angles are also observed, but are on the order of ~1–2°. In general, bond lengths and angles for **1** and **2** are similar to the comparable measurements for 4,4′-biimidazole with the expected differences at C2 and C8 (due to the absence of the methyl substituents).

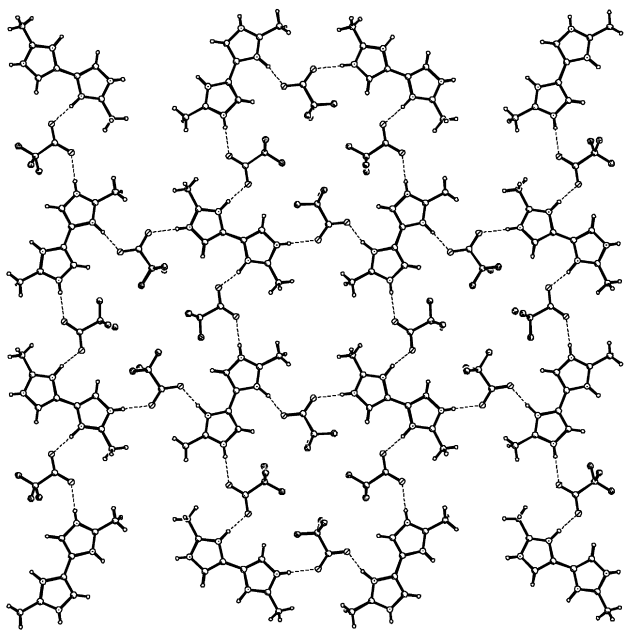

Figure 4. Packing diagram of **2** viewed parallel to the *c*-axis. Dashes lines represent hydrogen bonds. Only the major component of each disordered CF_3 group is shown.

Energy minimizations for the six isomers of **1** result in structures where the two 4,4′-biim rings are nearly coplanar as measured by the N1–C5–C6–C10 dihedral angle, which should be near zero degrees in the *S-trans* conformations and near 180° in the *S-cis* forms. *S-Trans* isomer **1a** shows a slightly higher degree of twisting (~20°) than is observed in the crystal structure of **1** while **1d** exhibits a large deviation from planarity (~−134°). Both of these isomers have protons attached to both nitrogen atoms and carbon atoms adjacent to the ring junctions, suggesting steric hindrance as the cause of the twisting. However, the highest energy form is **1f** (calculated to have a planar form), suggesting that this loss of planarity with its associated decrease in conjugation between the rings, does not cause large increases in energy for these isomers. The lowest energy form is the planar 1,9-*S-cis* isomer, **1e**. This results from the formation of an intramolecular interaction between the N–H proton of one ring and the unprotonated syn-nitrogen atom of the other ring. The calculated H1···N7 distance is relatively large

Table 4. Calculated geometries and energies for the tautomers and conformers of **1**

Structure	E_{calc} (Hartrees)	E_{rel}[a] (kcal/mol)	∠N1–C5–C6–C10 (°)
1a	−526.95333751	+2.75	20.1
1b	−526.95282066	+3.07	0.01
1c	−526.95771394	0.00	−0.03
1d	−526.94993043	+4.88	−133.8
1e	−526.95919755	−0.93	−179.997
1f	−526.94692308	+6.77	−179.998

[a] Relative to the energy of **1c**.

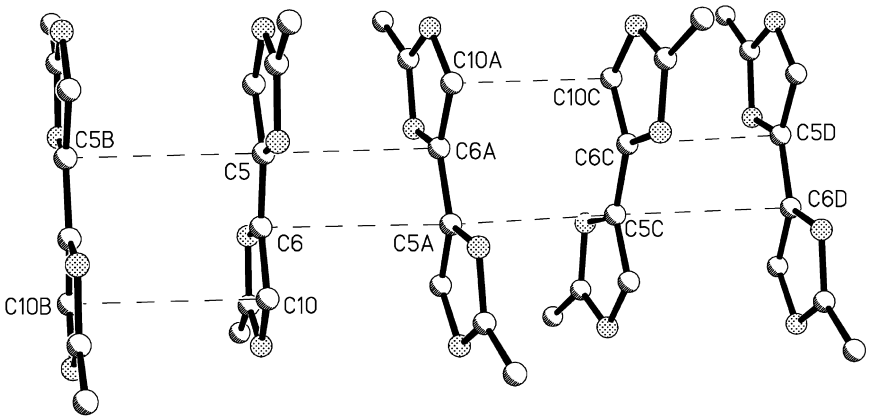

Figure 5. π-Stacking interactions between 4,4′-biimH$_2$ ions (*a*-axis vertical, *c*-axis ~horizontal). Dashed lines represent closest contacts between successive rings. Distances: C5–C5B═C5A–C5C=3.42 Å; C10–C10B═C10A–C10C=3.45 Å; C5–C6A═C6–C5A═C5C–C6D═C6C–C5D=3.44 Å.

(2.515 Å) and the angle unfavorable for a hydrogen bond, so the interaction may be dipolar in nature. However, the stabilization is clear from the bond angles at the ring junction (see Fig. 7). The two imidazole rings have been pulled toward each other, resulting in small N–C–C angles (<120°) on that side of the molecule. The corresponding angles in the other isomers of **1** are ~122–123°.

The isomer observed in the crystal structure, **1c**, is the next lowest in energy to **1e**. The presence of this isomer in the crystal structure, rather than **1e**, clearly results from the presence of water in the crystal lattice, forming hydrogen bonds as both donor and acceptor with all of the biimidazole nitrogen atoms. Calculated values for these hydrogen bonds (Table 3a) are in the range of −6–−10 kcal/mol, more than sufficient to overcome the small stabilization by the intramolecular hydrogen bond of **1e** in the anhydrous state.

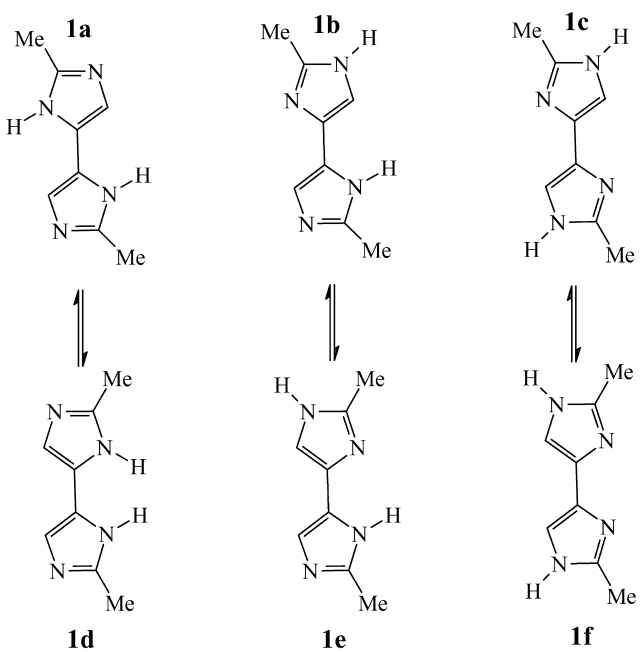

Figure 6. Theoretical tautomers and conformers of **1**.

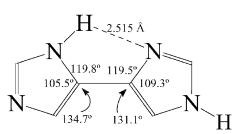

Figure 7. Data for the energy minimized structure of **1e**.

Interactions between the formula units of **2** that generate the extended planar structure are likely to result from two principle sources; ionic bonding and hydrogen bonding. The net interaction was estimated by comparing the calculated energy for the neutral formula unit (Fig. 3) with the energy for multiple formula units in their crystallographic positions. Each formula unit contains two acetate-biimidazole interactions (combination of ionic and hydrogen bonding), but as additional asymmetric units are added, an additional acetate-biimidazole interaction is introduced due to bridging by the acetate ions. This allows estimation of the interaction strength from the difference between the values calculated at their crystallographic positions relative to the same number of non-interaction formula units. The energy difference as a function of the number of bridging interactions is nearly linear (introduction of the 4th formula unit closes a circle, thus adding two additional acetate bridges) and independent of choice of cavity generated

Table 5. Calculations for 2,2′-dimethyl-4,4′-biimidazolium bistrifluoroacetate (**2**)

	Energy (eV)	ΔE^a (eV)	ΔE^a (kcal/mol)
Asymmetric unit	−1574.59897917		
Calculated energies for interacting asymmetric units[b]			
2 asym	−3149.23836426	−0.04040592	−25.4
3 asym	−4723.88115432	−0.08421681	−52.8
4 asym	−6298.56889987	−0.17298319	−108.65
Calculated energies for interacting asymmetric units[c]			
2 asym	−3149.23837559	−0.04041725	−25.4
3 asym	−4723.88127861	−0.08434110	−52.9
4 asym	−6298.57051187	−0.17459519	−109.6

[a] Relative to the equivalent number of non-interacting asymmetric units.
[b] To form the trifluoromethyl cavity.
[c] To form the methyl cavity.

(see Table 5). The resulting interaction energy is ~26 kcal/mol/bridge. The small increase in stabilization energy per unit as the number of formula units increases suggests that there are negligible contributions from extended molecular orbitals, supporting the original assumption that the significant interactions result from ionic and hydrogen bonding contributions. In like fashion, the similarity between the results for generation of the methyl lined cavity and the trifluoromethyl lined cavity suggests that van der Waals interactions are not significant contributors to the interaction energy.

4. Conclusions

We have solved the crystal structures for 2,2′-dimethyl-4,4′-biimidazole and 2,2′-dimethyl-4,4′-biimidazolium bis-trifluoroactate. Both compounds crystallize in *S-trans* conformations. Calculations show that these forms are stabilized by the presence of hydrogen bonding and/or ionic interactions in the lattice. Although this is not the conformation required for the formation of extended bimetallic coordination polymers, the calculated energy differences between the various conformations/tautomers are small and formation of the desired *S-cis* conformation should be facile. Work is in progress to prepare the desired metal complexes.

5. Experimental

5.1. Synthesis

Compound **2** was prepared according to the procedure of Cliff and Pyne[12] and used in the preparation of **1**. The identity and purity of the material was confirmed by mp, ^{1}H and ^{13}C NMR.

5.1.1. 2,2′-Dimethyl-4,4′-biimidazole dihydrate (1). Compound **2** (0.117 g, 0.3 mmol) was dissolved in 20 ml of H_2O. An aqueous solution of NaOH (0.2 M, 3.5 ml, 0.7 mmol) was added dropwise. The resulting solution was allowed to stand in the air at room temperature. After ~5 days, well-formed crystals were deposited. The crystals were collected by filtration and air-dried to give a pale yellow solid, 0.050 g (83%). Anal. for $C_8H_{14}N_4O_2$: calcd: C, 48.47; H, 7.17; N, 28.27. Found: C, 48.55; H, 6.93; N, 28.56. IR (KBr): ν 3314s, 3148s, 3065s, 2930s, 1681m, 1560s, 1415m, 1226m, 1156m, 1112m cm^{-1}. ^{1}H NMR (d_6-DMSO) δ 6.96 (br s, =CH) 3.45 (s, H_2O) 2.24 (s, CH_3).

5.2. Computational methods

All calculations were performed using the Gaussian-98 suite of programs.[17]

5.3. X-Ray crystallographic study

Data collection, cell refinement and data reduction for compounds (**1**) and (**2**) were done using a Bruker SMART/SAINT system[18] with Mo-radiation (λ=0.71073 Å) and a graphite monochromator at 168 K via φ and ω scans. The structures were solved via direct methods[19] and refined[20] via full-matrix least-squares. Absorption corrections were made via SADABS.[21] Hydrogen atoms bonded to N, or O atoms were located in the difference map and their positions refined with fixed, isotropic U's. Hydrogen atoms bonded to C atoms were placed in idealized geometric positions and refined using a riding model with fixed isotropic U's. Full crystallographic data may be found in Table 1. Selected bond lengths and angles are given in Table 2. Hydrogen bonding data are given in Table 3.

Crystallographic data for the structures reported in this paper have been deposited with the Cambridge Crystallographic Data Centre as supplementary publication no. CCDC-187213 (compound **2**) and CCDC-187214 (compound **1**). Copies of the data can be obtained from CCDC, 12 Union Road, Cambridge CB2 1EZ, UK [Fax: int. code +44-1223-336-033; e-mail: deposit@ccdc.cam.ac.uk].

Acknowledgements

Financial support from the NSF (DMR-9803813) and assistance with the X-ray data collection by Dr Jan Wikaira (U. of Canterbury) are gratefully acknowledged. In addition, M. M. T. received partial support as a Profesor Visitant from IBERDROLA (Programa 'Profesores Visitantes Iberdrola de Ciencia y Tecnología 2001-2003') and partial support from a grant from the Spanish Ministry of Science and Technology (Grant#SAB2000-0163).

References

1. See, for example (a). In *Magneto-structural Correlations in Exchange Coupled Systems*. Willett, R. D., Gatteschi, D., Kahn, O., Eds.; Reidel: Dordrecht, 1983. (b) In *Organic and Inorganic Low-dimensional Crystalline Materials*. *NATO ASI Series*; Drillon, P., Ed.; Plenum: New York, 1987. (c) In *Molecular Magnetic Materials*. *NATO ARW E198*; Kahn, O., Gatteschi, D., Miller, J. S., Palacio, F., Eds.; Kluwer: London, 1991. (d) In *Molecule-based Magnetic Materials: Theory, Techniques and Applications*. *ACS Symposium Series #644*; Turnbull, M. M., Sugimoto, T., Thompson, L. K., Eds.; American Chemical Society: Washington, 1996.
2. Decurtins, S.; Schmalle, H. W.; Schneuwly, P.; Ensling, J.; Gutlich, P. *J. Am. Chem. Soc.* **1994**, *116*, 9521.
3. Kahn, O.; Pei, Y.; Verdaguer, M.; Renard, J. P.; Sletten, J. *J. Am. Chem. Soc.* **1988**, *110*, 782.
4. Tamaki, H.; Zhong, Z.; Matsumoto, N.; Kida, S.; Koikawa, K.; Achiwa, N.; Hashimoto, Y.; Okawa, H. *J. Am. Chem. Soc.* **1992**, *114*, 6974.
5. Glynn, C. W.; Turnbull, M. M. *Inorg. Chim. Acta.* **2002**, *332*, 92–100.
6. Palmer, G.; Babcock, G.; Vickery, L. *Proc. Natl. Acad. Sci.* **1973**, *73*, 2006.
7. Cromer, D. T.; Ryan, R. R.; Storm, C. B. *Acta Crystallogr., Sect. C: Cryst. Struct. Commun.* **1987**, *43*, 1435.
8. Belanger, S.; Beauchamp, A. L. *Acta Crystallogr., Sect. C: Cryst. Struct. Commun.* **1996**, *52*, 2588.
9. (a) Ohrstrom, L.; Larsson, K.; Borg, S.; Norberg, S. T. *Chem.-Eur. J.* **2001**, *7*, 4805. (b) Lorente, M. A. M.; Dahan, F.; Sanakis, Y.; Petrouleas, V.; Bousseksou, A.; Tuchangues, J.-P.

Inorg. Chem. **1995**, *34*, 5346. (c) Haj, M. A.; Quiros, M.; Salas, J. M.; Dobado, J. A.; Molina, J. M.; Basallote, M. G.; Manez, M. A. *Eur. J. Inorg. Chem.* **2002**, 811. (d) Bencini, A.; Mani, F. *Inorg. Chim. Acta* **1988**, *154*, 215.

10. (a) Tadokoro, M.; Isobe, K.; Uekusa, H.; Ohashi, Y.; Toyoda, J.; Tashiro, K.; Nakasuji, K. *Angew. Chem., Int. Ed. Engl.* **1999**, *38*, 95. (b) Tadokoro, M.; Sato, K.; Shiomi, D.; Takui, T.; Itoh, K. *Mol. Cryst. Liqu. Cryst. Sci. Technol., Sect. A* **1997**, *306*, 49. (c) Tadokoro, M.; Daigo, M.; Isobe, K.; Matsumoto, K.; Nakasuji, K. *Mol. Cryst. Liqu. Cryst. Sci. Technol., Sect. A* **1997**, *306*, 391. (d) Tadokoro, M.; Kanno, H.; Kitajimi, T.; Shimada-Umemoto, H.; Nakanishi, N.; Isobe, K.; Nakasuji, K. *Proc. Natl Acad. Sci. U.S.A* **2002**, *99*, 4950.
11. Haddad, M. S.; Duesler, E. N.; Hendrickson, D. N. *Inorg. Chem.* **1979**, *18*, 141.
12. Cliff, M. D.; Pyne, S. G. *Synthesis* **1994**, 681.
13. Street, J. P. *Acta Crystallogr., Sect. C: Cryst. Struct. Commun.* **1991**, *47*, 411.
14. Stacking analysis performed using PLATON Spek, A. L. *Acta Crystallogr.* **1990**, *A46*, C–34.
15. Steel, P. J. In *Advances in Heterocyclic Chemistry*; Academic: New York, 1997; Vol. 67. pp 1–117.
16. (a) Morita, Y.; Murata, T.; Yamada, S.; Tadokoro, M.; Ichimura, I.; Nakasuji, K. *J. Chem. Soc., Perkin Trans. 1* **2002**, 2598. (b) Morita, Y.; Murata, T.; Yamada, S.; Tadokoro, M.; Nakasuji, K. *Mol. Cryst. Liq. Cryst., Sect. A* **2002**, *379*, 83.
17. Frisch, M. J.; Trucks, G. W.; Schlegel, H. B.; Scuseria, G. E.; Robb, M. A.; Cheeseman, J. R.; Zakrzewski, V. G.; Montgomery, J. A., Jr.; Stratmann, R. E.; Burant, J. C.; Dapprich, S.; Millam, J. M.; Daniels, A. D.; Kudin, K. N.; Strain, M. C.; Farkas, O.; Tomasi, J.; Barone, V.; Cossi, M.; Cammi, R.; Mennucci, B.; Pomelli, C.; Adamo, C.; Clifford, S.; Ochterski, J.; Petersson, G. A.; Ayala, P. Y.; Cui, Q.; Morokuma, K.; Malick, D. K.; Rabuck, A. D.; Raghavachari, K.; Foresman, J. B.; Cioslowski, J.; Ortiz, J. V.; Baboul, A. G.; Stefanov, B. B.; Liu, G.; Liashenko, A.; Piskorz, P.; Komaromi, I.; Gomperts, R.; Martin, R. L.; Fox, D. J.; Keith, T.; Al-Laham, M. A.; Peng, C. Y.; Nanayakkara, A.; Challacombe, M.; Gill, P. M. W.; Johnson, B.; Chen, W.; Wong, M. W.; Andres, J. L.; Gonzalez, C.; Head-Gordon, M.; Replogle, E. S.; Pople, J. A.; *GAUSSIAN 98* (release A.9); Gaussian, Inc.: Pittsburgh, PA, 1998.
18. Siemans *SMART* and *SAINT*: Area Detector Control and Integration Software; Siemans Analytical X-Ray Instruments, Inc., Madison, WI, USA, 1996.
19. Sheldrick, G. M. *SHELXS97*: Program for the Solution of Crystal Structures; University of Göttingen: Germany.
20. Sheldrick, G. M. *SHELXL97*: Program for the Refinement of Crystal Structures; University of Göttingen: Germany.
21. Sheldrick, G. M. *SADABS*: Program for Empirical Absorption Correction of Area Detector Data, 1996.